Open access • Journal Article • DOI:10.1103/PHYSREVB.79.134108

Mixed valency in cerium oxide crystallographic phases: Valence of different cerium sites by the bond valence method — Source link

Elvis Shoko, M. F. Smith, Ross H. McKenzie

Published on: 16 Apr 2009 - Physical Review B (American Physical Society)

Topics: Bond valence method, Cerium oxide, Valence (chemistry), Cerium and Valency

Mixed valency in cerium oxide crystallographic phases: Valence of different cerium sites by the bond valence method

E. Shoko, M. F. Smith, and Ross H. McKenzie
Department of Physics, The University of Queensland, Brisbane QLD 4072, Australia
(Received 25 November 2008; revised manuscript received 3 March 2009; published 16 April 2009)

We have applied the bond valence method to cerium oxides to determine the oxidation states of the Ce ion at the various site symmetries of the crystals. The crystals studied include cerium dioxide and the two sesquioxides along with some selected intermediate phases which are crystallographically well characterized. Our results indicate that cerium dioxide has a mixed-valence ground state with an *f*-electron population on the Ce site of 0.27 while both the *A*- and *C*-sesquioxides have a nearly pure f^1 configuration. The Ce sites in most of the intermediate oxides have nonintegral valences. Furthermore, many of these valences are different from the values predicted from a naive consideration of the stoichiometric valence of the compound.

DOI: 10.1103/PhysRevB.79.134108 PACS number(s): 61.72.jd, 61.68.+n

I. INTRODUCTION

The chemical concept of valence is of great utility.[1] The valence of an atom, *M*, determines the number of neighboring atoms with which *M* can form chemical bonds. For most metal ions, the valence, *V*, is equal to the oxidation number, *O*. Deviations from this equality occur when delocalization of electrons occurs. The simplest case is where *V* and *O* differ by one because one electron from each of the *M* atoms is completely delocalized in the conduction band. Mixed valency of transition-metal and rare-earth ions in solids and compounds is a question of fundamental interest in materials physics, chemistry, and molecular biophysics.[2] In 1967, Robin and Day[3] published a classification scheme for mixed valence that is still widely used today.[4] Class 1 describes systems with two crystallographic sites that are clearly distinct, and the two sites have integral but unequal valence. There is a large energy associated with transfer of electrons between sites. At the other extreme is class 3 for which there are two sites which are not distinguishable, and one assigns a nonintegral valence to both sites. The valence electrons are delocalized between the two sites. Class 2 is the intermediate case where the environments of the two sites are distinguishable but not very different. The energy associated with electron transfer is sufficiently small that it can be thermally activated and be associated with significant optical absorption in the visible range. On the time scale of the vibrations of the atoms, the electrons may appear to be delocalized. Classes 1 and 2 correspond to what Varma[5] terms as *inhomogeneous* mixed valence, although, perhaps, *inhomogeneous integral* valence may be more appropriate. Class 3 corresponds to *homogeneous* mixed valence.

In systems that are characterized by homogeneous mixed valence, each ion has the same noninteger valence which is a result of a quantum mechanical superposition of two integral valences occurring on each ion [see, for example, Eq. (2)]. Compounds exhibiting this type of mixed valence include, for example, $CePd_3$,[6] TmSe,[7] and SmB_6,[8] where the valences of the ions are 3.45, 2.72, and 3.7 for Ce, Tm, and Sm, respectively. In TmSe, the valence of 2.72 for the Tm ion is a result of valence fluctuations of this ion between the Tm^{2+} and Tm^{3+} states.[7] A distinctive experimental signature of homogeneous mixed valence is that the ground state is a spin singlet (and so has no net magnetic moment) even if one or both of the two oxidation states of the metal ion have a nonzero spin and magnetic moment.

In contrast to homogeneous mixed valence, the inhomogeneous mixed-valence case involves a mixture of different integer valence ions which occupy inequivalent lattice sites in a static charge-ordered array. Examples of this are provided by Fe_3O_4,[9] Eu_3O_4,[10] and Eu_3S_4.[11] The inverse-spinel crystal structure of magnetite (Fe_3O_4) is considered the classic case of inhomogeneous mixed valence. In this crystal, the Fe^{3+} ions completely occupy the tetrahedral (*A*) sublattice while the octahedral (*B*) sublattice is equally shared between the Fe^{3+} and Fe^{2+} ions and the ionic formulation is $(Fe^{2+})(Fe^{3+})_2(O^{2-})_4$. However, we note that this inverse-spinel charge ordering in Fe_3O_4 has recently been challenged in favor of the normal spinel charge structure where the Fe^{3+} ions exclusively occupy all the octahedral sites while the Fe^{2+} ions reside in the tetrahedral sites.[12] The crystal of Eu_3O_4 is a good example of the case where ions of different valence strictly occupy inequivalent cation sites. It consists of two nonequivalent Eu sites in which the Eu^{2+} and Eu^{3+} ions occupy the eight- and six-coordinated sites, respectively, giving a static charge-ordered array whose ionic formulation may be written as $(Eu^{2+})(Eu^{3+})_2(O^{2-})_4$.[10]

Oxides of cerium (Ce) appear to exhibit mixed-valence characteristics which may help to explain some of their properties relevant to their engineering applications. An important industrial use of Ce oxides is as anode materials in high-temperature solid-oxide fuel cells.[13] For these applications, CeO_2 (ceria) and Ce_2O_3 represent the extremal oxidation states in the reversible chemical reaction [Eq. (1)],

$$CeO_2 \rightleftharpoons CeO_{2-y} + \frac{y}{2}O_2, \quad 0 \le y \le 0.5. \tag{1}$$

Important questions concerning this system include: what is the origin of reversible uptake and release of oxygen by ceria? What is the origin and mechanism of the anionic conduction? What is the nature of oxygen vacancies in the bulk solid and on surfaces? When an oxygen atom is removed from a surface or crystal what happens to the two electrons

left behind? What is the nature, composition, and geometry of the catalytically active sites on cerium oxide surfaces?

A series of crystallographic phase transitions occurs between CeO_2 and Ce_2O_3, i.e., the reaction in Eq. (1). When CeO_2 is reduced to the various defective phases, CeO_{2-y}, O vacancies are formed in the lattice structure. The crystal structure adopted by any such defective phase, CeO_{2-y}, is understood to be the one that provides the most favorable energetics for the arrangement of all the O vacancies within the structure. In a widely accepted view of the microscopic description of O vacancy formation and ordering in CeO_{2-y} phases, the two electrons left by the O atom when an O vacancy forms fully localize on two of the nearest Ce^{4+} ions.[13–16] The localization of an electron on a Ce^{4+} ion converts it to the slightly larger Ce^{3+} ion with one electron in the $4f$ orbital. In the reverse process where a defective phase, CeO_{2-y}, is oxidized, two $4f$ electrons are transferred from the two neighboring Ce^{3+} ion sites into the O $2p$ band.

This description leads one to expect that the Ce lattice sites in the defective CeO_{2-y} phases would consist of a mixture of Ce^{3+} and Ce^{4+} ions in a static charge-ordered array. Thus, useful insight into the microscopic processes involved in the reversible chemical reaction [Eq. (1)] could be gained from knowledge of the valences of the Ce ions in the defective CeO_{2-y} phases. However, as we discuss in the Sec. II, it turns out that the task of establishing the oxidation states of the Ce ions in the lattices of the crystal phases involved in Eq. (1) is very challenging, owing to valence fluctuations on the Ce ions.

Here, we report the results of calculations based on a simple empirical method, the bond valence model (BVM),[17–19] to determine the valencies and, hence, the f-electron occupancies in the various Ce ion sites for seven of the crystallographic phases involved in Eq. (1). The crystals studied include A-Ce_2O_3, C-Ce_2O_3, Ce_3O_5, Ce_7O_{12}, $Ce_{11}O_{20}$, Ce_6O_{11}, and CeO_2.

The structure of this paper is as follows. In Sec. II we outline the general problem of mixed valence in Ce oxides from both experimental and theoretical perspectives. Section III describes the bond valence model and how we used it to determine the valences of Ce ions in the different phases of the Ce oxide crystals. We present our results in Sec. IV which we then discuss in light of two other models for predicting cationic valences in crystals. The main conclusions of this paper are given in Sec. V. Appendix A lists all the Ce-O bond lengths used in our calculations for Ce-centered polyhedra.

II. MIXED-VALENCE PROBLEM IN CERIUM OXIDES

In Ce oxides, the number of f electrons on a Ce site, N_f, is observed to lie between 0 and about 1.0. An isolated Ce atom has the electronic configuration $[Xe]4f^15d^16s^2$, a Ce^{4+} ion has [Xe], and Ce^{3+} has $[Xe]4f^1$. In a simple picture of ionic bonding in CeO_2 the Ce and O ions are both in closed shell configurations. This ionic picture can be justified if the $4f$ levels of the cerium are much higher in energy than the $2p$ levels of the oxygen. More precisely, the ionic picture will break down if the energy difference between the configurations f^0p^2 and f^1p^1 is less than the hybridization between these configurations.

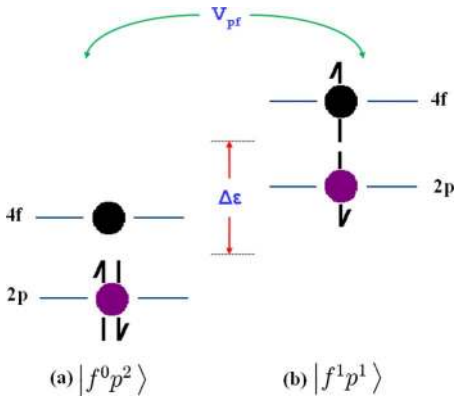

FIG. 1. (Color online) The schematic of the energy level structure of CeO_2 showing the two important system parameters in the Anderson impurity model: $\Delta\varepsilon$, the energy gap between the two states $|f^0p^2\rangle$ and $|f^1p^1\rangle$ which are mixed by the hybridization, V_{pf}. For CeO_2, the two parameters, $\Delta\varepsilon$ and V_{pf}, are comparable and the Ce $4f$ level may be close to the O $2p$ level (Ref. 20). In (a), the pure f^0 configuration corresponding to Ce^{4+} at the Ce site is shown. In (b), an electron has hopped from the O $2p$ site to the Ce site where it occupies the $4f$ level giving the pure f^1 configuration, i.e., Ce^{3+} as shown. An electron hole is thus created in the O $2p$ valence band. The mixing between these states due to the hybridization, V_{pf}, may result in mixed valence at the Ce site. Here, we have set the on-site Coulomb repulsion, U_{ff}, (for double occupancy of the f orbital) to infinity.

Figure 1 illustrates this situation for CeO_2 showing the relevant energy scales when the system is described by the Anderson impurity model.[20] Here, U_{ff}, the on-site Coulomb repulsion for the f orbital on a Ce site is considered to be very large. As already noted above, setting $U_{ff} \rightarrow \infty$ excludes from the ground-state wave function the state $|f^2p^0\rangle$ which corresponds to $N_f=2.0$. Once this assumption has been made, then, as shown in Fig. 1, the only key parameters of the model become the energy gap between the $|f^1p^1\rangle$ and $|f^0p^2\rangle$ configurations, $\Delta\varepsilon$, and the hybridization strength, V_{pf}.

Due to the mixing of states shown in Fig. 1, the electronic ground-state wave function of a Ce site in the oxide can be written in the general form as follows:

$$\Psi = \alpha|f^0p^2\rangle + \beta|f^1p^1\rangle, \tag{2}$$

where α and β are constants and $\alpha^2+\beta^2=1$, with the states assumed to be orthogonal. If for the two states $|f^0p^2\rangle$ and $|f^1p^1\rangle$, $\Delta\varepsilon$ and V_{pf} are comparable, then the necessary conditions for valence fluctuation phenomena hold.[5,21] Thus one can think of the $4f$ level at a given Ce site as fluctuating between the f^0 and f^1 configurations.

Various experimental and theoretical approaches have been brought to bear on the problem of mixed valence in Ce oxides with much of the focus concentrated on CeO_2 and to some extent Ce_2O_3. There appears to be general agreement that the electronic ground state of Ce_2O_3 is the f^1 configuration.[22,23] However, controversy exists on the exact nature of the ground state of CeO_2 with strong arguments in

favor of both a pure f^0 configuration and a mixed-valence ground state. We briefly review a bit of this interesting debate indicating which approaches have consistently arrived at the same conclusions and which ones have had mixed interpretations.

A. Experiment

The $3d$ photoabsorption and photoemission spectra analyzed by the Anderson impurity model consistently reach the conclusion that CeO_2 has a mixed valent ground state.[20,22–27] A cluster model has also been used to interpret some $3d$ photoemission spectra, and it was also concluded that the f state is strongly mixed valent in the ground state of CeO_2.[28,29] Although the results of $3d$ x-ray photoemission spectroscopy (XPS), interpreted in the Anderson impurity model, have consistently predicted a mixed-valent ground state for CeO_2, doubts have been raised about the reliability of assigning initial state configurations from Ce $3d$ XPS spectra because of the possibility of reduction of the oxide on exposure to the x-ray radiation.[30] Perhaps an even more difficult challenge in the interpretation of XPS spectra is how to trace the ground-state configuration of a sample from the spectral signatures of the final state of XPS. The conventional interpretation is that in Ce_2O_3, the two-peak structure observed in XPS spectra is a result of final state effects whereas CeO_2 shows a three-peak structure in its XPS spectrum which has been attributed to final state effects.[20,22,23]

X-ray absorption near-edge spectroscopy (XANES) has provided a second source of evidence for the mixed valence of the ground state of CeO_2. The characteristic double peak structure observed in all XANES spectra is considered a signature for mixed valence in CeO_2.[31–38]

In contrast to the $3d$ XPS and XANES data discussed above, the $4d$-$4f$ photoabsorption spectra of CeO_2 support the f^0 ground-state configuration based on their close resemblance to La trihalide spectra which have no f electron while they differ considerably from the Ce trihalide spectra which have one f electron.[39,40] Also in favor of the f^0 ground-state configuration are results from reflectance spectroscopy in the $4d$-$4f$ absorption region.[41]

Among the methods which have produced an ambiguous picture of the ground state of CeO_2 are included resonant inelastic x-ray spectroscopy (RIXS), bremsstrahlung isochromat spectroscopy (BIS), valence-band XPS, and energy band structure calculations. Application of resonant photoemission to the problem led to the conclusion that the ground state of CeO_2 is mixed valent by some authors[42,43] while a pure f^0 configuration was claimed by others.[39,40,44] The spectrum investigated by the BIS combined with XPS study shows empty localized $4f$ states in the band gap providing evidence in support of the pure f^0 configuration.[24,45] This conclusion was also supported by valence-band XPS studies.[46,47] However, it was later shown that the valence-band photoemission, BIS, and $4d$ photoabsorption spectra can all be explained consistently with other core-level spectra by the Anderson impurity model.[27,48,49] The results of this analysis led to the conclusion that CeO_2 is mixed valent in the ground state.

B. Electronic structure calculations

An energy band calculation by the linear augmented plane wave (LAPW) method showed a $4f$ electron count of ~ 0.5 with considerable covalent character.[50] Similar results were obtained from a linear muffin-tin orbital (LMTO) band structure[36] and in a molecular orbital calculation of a CeO_8 cluster.[51] On the other hand, band structures of CeO_2 obtained from density-functional theory (DFT) calculations, both in the local density approximation (LDA) and generalized gradient approximation (GGA), have empty $4f$ states above the valence band supporting the f^0 ground-state configuration.[52–55] This electronic configuration for CeO_2 is widely accepted in DFT work largely because it predicts the structural properties of the CeO_2 crystal with reasonable accuracy. However, LDA and GGA predict a ferromagnetic metal ground state rather than the experimentally observed insulating ground state of Ce_2O_3. This is because these functionals do not yield a proper localization of the f electrons on the Ce sites. Some pragmatic strategies have been adopted to augment LDA and GGA so that predictions closer to the experimental results could be obtained. Skorodumova *et al.*[55] artificially localized the $4f$ states in what was called the "core state model." Others have used the LDA(GGA)$+U$ formalism, where an onsite Coulomb repulsion is incorporated to account for the repulsive energy arising from the double occupancy of an f orbital on a Ce site.[53,56,57]

Hybrid functionals consist of a linear combination of LDA (GGA) and the Hartree-Fock (HF) exchange function. They have been applied to both CeO_2 and Ce_2O_3 and are a significant improvement on LDA (GGA) as both the predicted structural properties and the qualitative features of the band structures are correct. Specifically, insulating ground states are obtained for both CeO_2 and Ce_2O_3 along with the experimentally observed antiferromagnetic coupling for the latter. However, the band gaps are overestimated relative to experiment.[52,58] As Brothers *et al.*[59] noted, the fact that band gaps from screened hybrid functionals are qualitatively correct should not be a surprise since they are constructed from a combination of semilocal functionals which underestimate band gaps and an exchange of the Hartree-Fock-type which overestimates them.

An electronic structure method which arguably gives a more reliable description of the electronic correlations and does not require the use of hybrid functionals is based on combining dynamical mean-field theory with density-functional theory.[60] An implementation which takes into account in a self-consistent manner how correlations modify the charge density and thus the effective Kohn-Sham Hamiltonian has been reported.[61]

III. BOND VALENCE MODEL

The BVM, which is a generalization of Pauling's original concept of the electrostatic valence principle, has been reviewed extensively in the literature.[17–19] A quantum chemical justification of the model has been discussed by Mohri.[62] The concept of bond valence has worked well for many oxides. Brese and O'Keeffe[63] showed how it can describe more than 30 different metal-oxygen bonds and give the corresponding bond valence parameters. They mentioned briefly that Cu(III)-O bonds may have less than their formal valence. In the case of lanthanide-oxygen bonds, a detailed analysis was

given by Trzesowska *et al.*[64] and no problems were noted in applying the model to these bonds.

The BVM defines the relationship between bond valences, s, and the corresponding atomic valences, V, through the following equation:

$$V_i = \sum_j s_{ij}, \tag{3}$$

where i and j refer to different atoms sharing a bond. This relationship is called the valence-sum rule.

There is a well-defined empirical relationship between bond valences as defined in Eq. (3) and bond lengths in a given coordination polyhedron, and it is this functional relationship which makes the BVM quantitatively useful. The relationship is monotonic, and over the small range in which most bonds are found, it can be approximated by[18]

$$s_{ij} = \exp\left(\frac{R_0 - R_{ij}}{B}\right). \tag{4}$$

Here R_0 and B are fitted parameters, R_0 being the bond length of a bond of unit valence. For a specific bond, these parameters are determined by fitting the measured lengths of bonds in a wide range of compounds by enforcing the valence-sum rule Eq. (3). It has been shown that for most bonds, B can actually be set to be 0.37 Å which reduces the bond valence model Eq. (4) to a one-parameter model.[63] In that case, for each structure where a central atom is bonded only to atoms of a particular species, the R_0 parameter is then obtained by combining the valence-sum rule Eq. (3) and Eq. (4); i.e.,

$$V_i = \sum_j s_{ij} = \sum_j \exp\left(\frac{R_{0i} - R_{ij}}{B}\right) = \exp\left(\frac{R_{0i}}{B}\right)\sum_j \exp\left(\frac{-R_{ij}}{B}\right), \tag{5}$$

which can be rewritten in the following form:

$$R_{0i} = B \ln\left[\frac{V_i}{\sum_j \exp\left(\frac{-R_{ij}}{B}\right)}\right]. \tag{6}$$

The BVM is applicable to *bipartite* crystals which, in our case, means that only Ce-O bonds can exist in any given crystal. In all cases, the bipartite requirement is satisfied for Ce polyhedra considered below. However this is not true for all O polyhedra as in a few cases, e.g., in Ce_6O_{11}, O atoms are included in the coordination polyhedron of an O atom. Nevertheless, this does not concern us as all our calculations are performed on cation-centered polyhedra. A second issue arises from how to precisely define the coordination number for some of the Ce sites. The general problem of calculating coordination numbers of low-symmetry sites in inorganic crystals is well known.[65–68] Several different formulae and inputs to the calculation have been suggested to determine effective coordination numbers (ECoNs) in the low-symmetry sites.[67,69–71] The ECoNs listed in Table I have been calculated from the method suggested by Hoppe *et al.*[70]

For the purpose of our bond valence calculations, we adopt the definition of Brown[72] of the coordination number as the number of atoms (O, in this case) to which a central atom (Ce, in this case) is bonded.[72] An operational meaning of this definition was given by Altermatt and Brown:[73] a bond exists between a cation and an anion if its experimental bond valence is larger than 0.04× the cation valence. The Ce coordination polyhedra in all the oxides were well defined by the definition of Brown[72] except for the case of Ce_6O_{11} where there were ambiguities in delineating the various Ce polyhedra. It was, in fact, only in this instance that the Brown-Altermatt criterion[73] was actually necessary in order to exclude some marginal bonds from the first coordination sphere. The case of Ce_6O_{11} is discussed further in Sec. IV.

Various authors have determined values for parameters R_0 and B in Eq. (4) for Ce-O bonds from an analysis of measured bond lengths in both organic[64,74] and inorganic compounds.[63,75] It has been reported that Ce-O bonds in inorganic compounds are longer than in metal-organic coordination compounds and so the bond parameters are larger.[64] Although Zocchi[75] derived detailed parameters for the Ce-O bonds in inorganic compounds explicitly giving the dependence on coordination number, his so-called method of intercepts[76] does not provide a clear physical basis for the calculation. In view of these considerations, we selected the parametrization of the BVM by Brese and O'Keeffe.[63]

In this parametrization, $B=0.37$ Å with $R_0=2.151$ Å and $R_0=2.028$ Å for Ce^{3+} and Ce^{4+} ions, respectively. This means that by the criterion of Brown[72] for the coordination sphere, only O atoms within the critical distances $R_c=2.905$ Å and $R_c=2.746$ Å are included within the coordination polyhedron for Ce^{3+} and Ce^{4+} sites, respectively.

We briefly summarize the main crystallographic information for all the crystal structures studied in this work. For each crystal structure, we provide the space and crystal point groups as well as the number of formula units in the unit cell. Individual site symmetries are given in Table I, and for more detailed crystallographic data about the structures, the references in this table should be consulted.

The two well-known oxides of Ce are the dioxide, CeO_2, and the sesquioxide, A-Ce_2O_3. The CeO_2 crystal is a fluorite structure, space group $Fm\bar{3}m$, and point group O_h with 4 f.u./unit cell. The A-sesquioxide has a hexagonal lattice with 1 f.u./unit cell, and its structure belongs to the space and point groups, $P\bar{3}m1$ and D_{3d}, respectively. In contrast, the C phase of Ce_2O_3 has a body-centered cubic lattice, space group $Ia\bar{3}$, and point group T_h. There are 16 f.u./unit cell of C-Ce_2O_3. Except for the partial (39%) occupancy of the Wyckoff 16c sites by additional O atoms, Ce_3O_5 has exactly the same structure as C-Ce_2O_3. The unit cell consists of 11 (32/3) f.u.. Ce_7O_{12} has a rhombohedral lattice (a hexagonal setting can also be used), space group $R\bar{3}$, point group C_{3i}, and 3 f.u./unit cell. Of all the structures studied here, $Ce_{11}O_{20}$ is the least symmetrical with only inversion as its point group symmetry and has the space group $P\bar{1}$ and 1 f.u./unit cell of the crystal. Lastly, Ce_6O_{11} has a monoclinic lattice consisting of 4 f.u. in the unit cell. The space and point groups are $P2_1/c$ and C_3, respectively.

To perform bond valence calculations, the only input required is the bond length data of the Ce-O bonds in the respective coordination polyhedra of the various oxides. For

TABLE I. Site valencies of Ce at different sites in cerium oxides (CeO_{2-y}) calculated from our self-consistent bond valence method.

Oxide	y	Ref.	Ce site	CN[a]	ECoN[b]	Symm.[c]	Sites[d]	SBVS (v.u.)[e]	N_f [f]	% Var.[g]
A-Ce_2O_3	0.50	82 and 83	Ce	7	5.7	C_{3v}	2	2.97	1.03	14
C-Ce_2O_3	0.50	83–85	Ce(1)	6	6.0	S_6	8	3.01	0.99	0.0
			Ce(2)	6	6.0	C_2	24	2.97	1.03	3.5
Ce_3O_5	0.33	83, 85, and 86	Ce(1)	6.78[h]	6.6	S_6	8	3.22	0.78	9.0
			Ce(2)	6.78[h]	7.7	C_2	24	3.22	0.78	5.0
Ce_7O_{12}	0.29	87 and 88	Ce(1)	6	6.0	S_6	3	3.67	0.33	0.0
			Ce(2)	7	6.5	1	18	3.21	0.79	7.0
$Ce_{11}O_{20}$	0.18	85 and 89	Ce(1)	8	7.3	$\bar{1}$	1	3.08	0.92	13
			Ce(2)	8	7.6	1	2	3.06	0.94	7.6
			Ce(3)	7	6.8	1	2	3.46	0.54	7.8
			Ce(4)	7	6.6	1	2	3.58	0.42	12.5
			Ce(5)	7	6.8	1	2	3.68	0.32	8.2
			Ce(6)	7	6.8	1	2	3.76	0.24	9.4
Ce_6O_{11}	0.17	80, 84, and 90	Ce(1)	6	4.6	1	4	3.22	0.78	30.9
			Ce(2)	7	5.0	1	4	3.75	0.25	26.7
			Ce(3)	7	5.8	1	4	3.10	0.90	15.1
			Ce(4)	5	7.0	1	4	3.62	0.38	37.4
			Ce(5)	6	5.0	1	4	2.93	1.07	24.0
			Ce(6)	6	6.1	1	4	3.22	0.78	30.9
CeO_2	0.00	80, 84, and 91	Ce	8	8.0	O_h	4	3.73	0.27	0.0

[a]The coordination of a Ce site determined from the Brown-Altermatt criterion (Ref.73).
[b]The effective coordination number of a Ce site determined from the formula of Hoppe *et al.* (Ref. 70).
[c]The local symmetry at a cerium site.
[d]The total number of Ce sites of a specified site symmetry in the unit cell of the crystal.
[e]The site bond valence sum (SBVS) calculated self-consistently by the bond valence method and given in valence units (v.u.).
[f]N_f is the occupation of the $4f$ orbital on a Ce site and is calculated self-consistently by the bond valence method.
[g]% Var. refers to the variation in bond lengths for a given polyhedron and this quantity is calculated from Eq. (12).
[h]The noninteger coordination number is a result of the partial (39%) occupation of the Wyckoff 16c sites of this crystal.

this, we obtained crystallographic data from the sources listed in Table I. For each oxide, all the distinct coordination spheres for both Ce and O atoms were identified. Figure 2 illustrates the procedure using the example of Ce_7O_{12} where we have shown only one of the two O atom polyhedra in the crystal of this oxide. The Ce-O bond distances in each polyhedron were then obtained from the crystallographic data using CrystalMaker.[77] We have listed the Ce-O bond length data in Appendix A. We note here two oxides, C-Ce_2O_3 and Ce_6O_{11}, for which we were not able to obtain full crystallographic data. C-Ce_2O_3 has not been observed experimentally and the lattice constant used here, 11.22 Å, was estimated by Eyring[78] and also by Tsunekawa *et al.*[79] We could not find positional parameters for the crystal of Ce_6O_{11}, and we used the positional parameters for Pr_6O_{11} with which it is isostructural.[80]

The relationship among valence, oxidation number, and orbital occupation is subtle. "Unusual valence" occurs when there is a difference between the oxidation number and the "localized" valence.[81] Such a difference occurs in rare-earth halides such as Pr_2Br_5 and is associated with multicenter bonding and "configuration crossovers" between $f^n d^0$ and $f^{n-1}d^1$. The paper of Mohri[62] on the quantum chemical justification of the bond valence model establishes a connection between the valence and the orbital occupation of an ion.

IV. RESULTS AND DISCUSSION

We have noticed from the results of Roulhac and Palenik[74] that the parameter R_0 varies approximately linearly with the oxidation state of the Ce atom between R_0 =2.121(13) Å (Ce^{3+}) and R_0=2.068(12) Å (Ce^{4+}). We exploit this relationship between R_0 and the Ce oxidation state to calculate the f occupancies of the Ce sites self-consistently in the following way. As already mentioned, the valence at each Ce site fluctuates between the $f^0(Ce^{4+})$ and $f^1(Ce^{3+})$ configurations. Let x be the probability that a Ce ion is in the f^1 configuration ($0 \le x \le 1$); then, the corresponding probability of the f^0 configuration at the same site is given by $1-x$. Thus, for such a mixed-valence Ce site, the corresponding value of the parameter R_0 is then given by linear interpolation between these values,

$$R_0 = R_3^0 x + R_4^0 (1-x). \tag{7}$$

As already mentioned, we have used R_3^0=2.151 Å and R_4^0 =2.028 Å, i.e., R_0 parameters for Ce^{3+} and Ce^{4+} states,

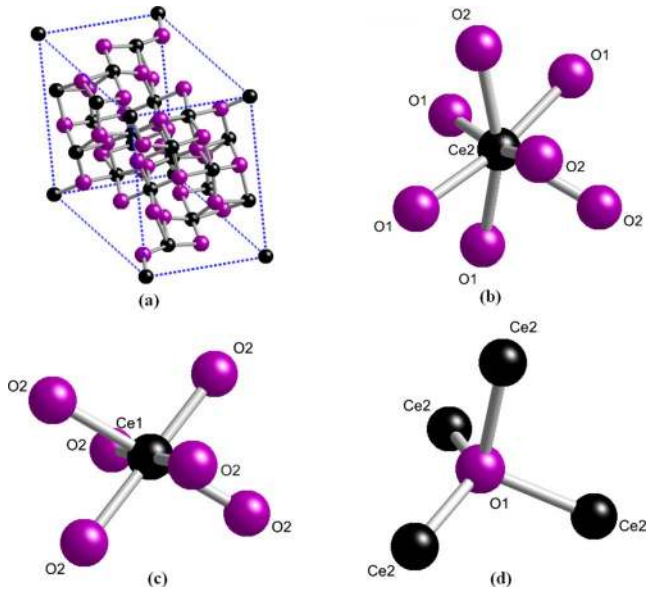

FIG. 2. (Color online) Identification of the coordination polyhedra in Ce_7O_{12} for bond valence calculations. Atom labels refer to the distinct sites in the crystal. (a) The unit cell of Ce_7O_{12} in the hexagonal crystal lattice. The space group is $R3$, and the unit cell consists of 3 f.u. (b) The polyhedron of the Ce(2) site which is seven coordinated and of triclinic symmetry and (c) that of the six-coordinated Ce(1) site of S_6 symmetry. There are two distinct polyhedra for the O atoms, and one of these [the O(1) site] is shown in (d). In this polyhedron, the O atom has a coordination of four in triclinic symmetry. The colors of the atoms are: Ce: black (black); O: black (violet). Images are generated in CRYSTALMAKER (Ref. 77).

respectively.[63] From Eqs. (7) and (4), we have

$$s_{ij}(x) = \exp\left(\frac{[R_3^0 x + R_4^0(1-x)] - R_{ij}}{B}\right). \tag{8}$$

It then follows that, for a Ce site i, $V_i(x)=4-x=\sum_j s_{ij}(x)$, which then with $N_f=x$, leads to the required self-consistent equation,

$$x = 4 - \sum_j \exp\left(\frac{[R_3^0 x + R_4^0(1-x)] - R_{ij}}{B}\right). \tag{9}$$

We solved Eq. (9) for $x=N_f$ to get the f occupancies of the various Ce sites in the seven crystals studied. The results of applying Eq. (9) to the seven oxides of cerium selected for this study are given in Table I.

For CeO_2, all O atoms are symmetry equivalent (as are all Ce atoms). For this simple case, we can write down an equation describing the polyhedron centered on a given O, equivalent to Eq. (9), and use it to determine the valence of the O atom self-consistently. The valence on the oxygen atom of CeO_2 is given by

$$V_i(x) = -1.5x - 2(1-x) = \sum_{i=1}^{4} s_{ji}(x) = -\sum_{i=1}^{4} s_{ij}(x)$$

$$= -\sum_{i=1}^{4} \exp\left(\frac{[R_3^0 x + R_4^0(1-x)] - R_{ij}}{B}\right) \tag{10}$$

$$\Rightarrow x = 4 - 2\sum_{i=1}^{4} \exp\left(\frac{[R_3^0 x + R_4^0(1-x)] - R_{ij}}{B}\right). \tag{11}$$

Evaluation of Eq. (11) gives $x=0.268$ from where it follows that the O valence is -1.87 which is consistent with the Ce valence already calculated above.

In the general case, in which there are inequivalent O atoms, we cannot determine the valence of a given O site in this way. That is, while the valence of each Ce atom can be determined by considering the polyhedron consisting of this central Ce and its nearest neighbors, the same is not generally true for an O atom. This is because we have assumed that the parameter R_0, a property of a Ce-O bond, depends on the valence of the Ce atom but not on the valence of the O atom. This assumption is consistent with the observation that the structures of different Ce oxides with the same Ce valence can be adequately described by Eq. (4) using a single value for R_0.[92]

Locock and Burns[93] defined a measure of the variation in bond lengths of the bonds included in a coordination polyhedron as follows:

$$\text{variation}(\%) = \frac{|\text{bond}_{\max} - \text{bond}_{\min}|}{\text{bond}_{\text{avg}}} \cdot 100, \tag{12}$$

where the subscripts max, min, and avg refer to the maximum, minimum, and average bond lengths in the polyhedron. We have calculated the percent variation for all the polyhedra in this study, and the results are given in Table I.

We now give a few remarks about the accuracy of the bond valence method. Brown[92] estimated that bond valence sums have an accuracy of 0.05 v.u. The main error in the method comes from the fitted parameters of the model (B,R_0). It has been noted that bond valence parameters which overestimate valences of strong bonds while underestimating those weak bonds will give bond valence sums which are too high in low coordination polyhedra and too low in the case of high coordination.[94] We have estimated that with the following uncertainties in the model parameters and bond length data, $R_0(\pm 0.01$ Å), $R_{ij}(\pm 0.01$ Å),[63] and $B(0.037$ Å),[18] the uncertainties in the bond valence sums for CeO_2 and A-Ce_2O_3 are ± 0.13 and ± 0.12 v.u., respectively, which is in agreement with Ref. 95.

In Fig. 3, we have plotted the Ce site f occupancies, N_f, calculated from Eq. (9). The results are plotted for increasing average degree of oxidation of the Ce ion. For each crystal, the results are reported according to the site symmetries of the Ce sites which range from the lowest triclinic sites (i) to the most symmetrical octahedral sites (O_h). The dashed line labeled Ce_2O_3 refers to both the A and C phases of this oxide. For comparison, we have included the solid straight

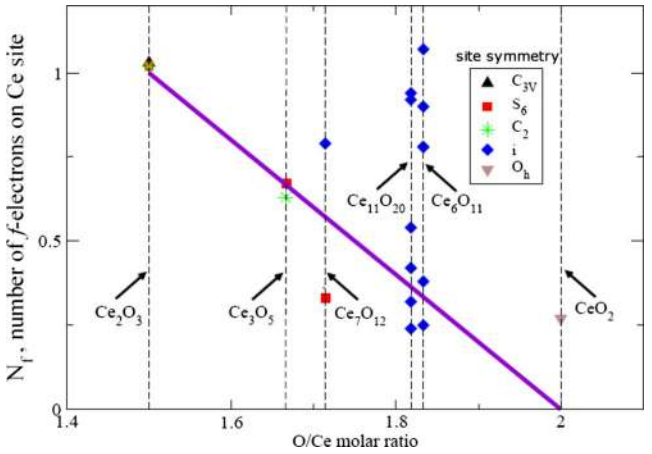

FIG. 3. (Color online) Ce f-level site occupancies in different crystallographic phases of the oxides calculated self-consistently in the bond valence model. The results are given according to the exact point group symmetries of the respective Ce sites in each crystallographic phase. As can be seen from the legend, the point symmetries of the Ce sites vary from as low as triclinic (i) to as high as octahedral (O_h), the point group of the cube. The straight line represents N_f values obtained from a simple Ce valence calculation based on the electroneutrality of the formula unit and the assumption of an oxidation state of −2 for the O ions in all the oxides.

line which represents N_f values calculated from the formula units by requiring charge balance of the formula unit, a valence of −2 for all O ions, and an even distribution of the valence among all the Ce ions in a formula unit. We will call this method of calculating N_f the homogeneous mixed-valence approximation (HMA) as it assigns the same valence to each cationic site regardless of the specific site properties. We contrast this method with another simple approach for predicting cationic valences which we will call the inhomogeneous mixed-valence approximation (IHMA). The IHMA is based on the requirement that all valences must be integral, but their exact assignment in the crystal lattice does not necessarily have to satisfy constraints which may arise from specific differences in local site symmetry. Thus, this approximation considers the crystal lattice to be a static charge-ordered array.

The results plotted in Fig. 3 show that mixed valence in Ce oxides does not fit nicely into either of the traditional classes of mixed valence, i.e., homogeneous or inhomogeneous mixed valence as originally defined by Varma.[5] For the Ce oxides, only CeO_2 and Ce_2O_3 are strictly homogeneous mixed-valent oxides since all the Ce sites are symmetrically equivalent and have the same oxidation state. The rest of the oxides do not have symmetrically equivalent Ce sites, and the oxidation states of the individual sites are generally different within the error limits of the method. The mixed valence in the crystal is not a result of the averaging of the oxidation states at the different sites but a property of the individual sites, which means that the mixed valence is not of the simple inhomogeneous type.

It is interesting and important to compare our results to those obtained by other methods. In Table II we have reported the results of the Ce site 4f occupancy, N_f, from the literature. We have not been able to obtain results for all other oxides except for CeO_2 and Ce_2O_3. The data in Table II show that while there is good agreement on the f occupancy of the Ce site in A-Ce_2O_3, there is considerable variation in the reported results for CeO_2. The N_f values for CeO_2 vary from 0.00 for LDA and GGA calculations to 0.60 for Ce 3d core XPS. We now discuss our results in detail for the individual oxides. The format of our discussion is as follows: for each oxide, we compare the predicted valences from the BVM to those obtained from HMA and IHMA. We then indicate whether or not the particular oxide exhibits mixed valence.

A. A-Ce_2O_3

The bond valence method gives N_f=1.0 for this oxide. As can be seen from Table II, the bond valence method gives N_f values which accord well with results from the other methods for this oxide. In addition, both the HMA (Fig. 3) and IHMA also predict N_f=1.0 and so all the methods are in agreement. Compared to CeO_2, Table II shows that the variation in bond lengths in the Ce polyhedron of A-Ce_2O_3 is relatively high at about 14%. However, the result of N_f obtained in this calculation which is in good agreement with other methods may suggest that bond length distortions of this magnitude may have no significant role in the bond valence model. We conclude that mixed valence in A-Ce_2O_3 is negligible.

B. C-Ce_2O_3

The results are similar to those for A-Ce_2O_3 just described above in both the S_6 and C_2 site symmetries of C-Ce_2O_3. However, structurally, the two sesquioxides are very different. The A-sesquioxide has a hexagonal Bravais lattice (space group $P\bar{3}m1$) with lattice constants a=3.891 Å and b=6.059 Å and only one Ce site of C_{3v} symmetry. In contrast, the C-sesquioxide has a cubic fluorite structure with two O vacancies along the body and face diagonals (space group $Ia\bar{3}$) giving the S_6 and C_2 site symmetries for the Ce ions, respectively. That the Ce sites in A-Ce_2O_3 and C-Ce_2O_3 still have the same N_f value despite the differences in point symmetry appears to suggest that site symmetry may have no significant influence on the valence of a given site in Ce_2O_3. Compared to the other oxides included in this study, the only other Ce site with a comparable N_f value is the triclinic Ce(5) site in Ce_6O_{11}.

C. Ce_3O_5

The results in Table I indicate that both Ce sites in this crystal have the same valence and the N_f value is 0.78. Again, this result highlights the earlier observation that site symmetry may have no significant role in site valences since the two Ce sites have the same valence although their symmetries are different. The HMA predicts that N_f=0.67 for this crystal which is somewhat lower than the BVM value, while the IHMA requires the ionic formulation $[(Ce^{3+})_2Ce^{4+}](O^{2-})_5$ for Ce_3O_5. Thus, the IHMA indicates that in a static charge-ordered array of integral valences, the

TABLE II. Values for the $4f$ orbital occupation, N_f, on the Ce ion in various cerium oxides. The table compares values determined by different experimental and theoretical methods.

Compound	N_f	Method	Remarks	Ref.
CeO_2	0.3 ± 0.1	Bond valence	From crystal structure data	This work
	0.60	Ce $3d$ core XPS	Bulk measurement	28
	0.45	XANES	Bulk measurement	96
	0.50	Ce $3d$ core XPS	Bulk measurement	20
	0.1–0.35	Ce $2p$ XAS	Bulk measurement	97
	0.05	Optical reflectance	Bulk, measurement	98
	0.2–0.4	LDA+U	Bulk, calculation	99
	0.50	LAPW χ_α	Bulk, calculation	50
	0.40	Ce $3d$ XAS	Bulk, calculation	100
	0.20	HSE[b]	Bulk, calculation	52 and 58
	0.00	LDA and GGA	Bulk, calculation	55
Ce_2O_3	1.0 ± 0.1	Bond valence	From crystal structure data	This work
	1.0	Ce $3d$ core XPS	Bulk measurement	20
	1.0	LDA and GGA[a]	Bulk, calculation.	55
	1.0	HSE[b]	Bulk, calculation	52 and 58
	1.17	DMFT-SC[c]	Bulk, calculation	61
$Ce_2Zr_2O_{7.5}$	0.5	EELS (Ce-$M_{4,5}$)	Bulk measurement, ceria-zirconia solid solution	101

[a]Both the LDA and GGA calculations were performed by artificially localizing the $4f$ states, the so-called core state model. Hence, $N_f=1$ was actually assumed in the calculation.
[b]HSE denotes a particular hybrid functional.
[c]DMFT-SC denotes dynamical mean-field theory with self-consistent charge density

Ce_3O_5 lattice has twice as many Ce^{3+} ions as Ce^{4+} ions. Although the Ce(1) and Ce(2) sites are of different point group symmetries, they are of comparable polyhedron sizes with average Ce-O distances of 2.4354 and 2.4110 Å, respectively. When one considers how to distribute the Ce^{3+} and Ce^{4+} ions between these sites, there is a conceptual difficulty. First, in typical ionic crystals of Ce, the average radii of the ions in an eight-coordinate environment are 1.28 and 1.11 Å for Ce^{3+} and Ce^{4+}, respectively.[102] For a six-coordinate environment, the same radii are 1.15 and 1.01 Å, respectively. Thus the average difference in the crystal radii of the cations is 13% in Ce_3O_5 where the coordination number is 6.78. This difference in the crystal radii of the ions is significantly different from the 1.0% difference in the average sizes of the coordination polyhedra. Second, the ratio of the Ce(1) and Ce(2) sites does not match that of the ions as given in the ionic formulation above. Thus, if one were to argue that the smaller Ce^{4+} ion will show a slight preference for the smaller Ce(2) site, then all the Ce^{4+} ions would occupy the Ce(2) sites. However, since there are almost twice as many Ce(2) sites as Ce^{4+} ions, the remainder of these sites will be occupied by the Ce^{3+} ions and the latter will, in addition, occupy all the Ce(1) sites. This, of course, results in a situation where Ce^{3+} and Ce^{4+} occupy the same type of site in the crystal. This logical inconsistency does not arise when the BVM is applied, and we conclude that Ce_3O_5 is a homogeneous mixed-valence compound.

D. Ce_7O_{12}

Both the Ce(1) and Ce(2) sites are predicted in the BVM to be mixed valent with the more symmetrical Ce(1) site closer to Ce^{4+} (3.67 v.u.) and the triclinic Ce(2) site closer to Ce^{3+} (3.21 v.u.) whereas the HMA gives a valence of 3.4 v.u. The ionic formulation for the IHMA is $[(Ce^{3+})_4(Ce^{4+})_3](O^{-2})_{12}$ giving the unit cell, $[(Ce^{3+})_{12}(Ce^{4+})_9](O^{-2})_{36}$ for Ce_7O_{12}. The Ce(1) site is smaller than the Ce(2) site, and it has been suggested that since the lower coordination at the Ce(1) site would require a smaller cation, then Ce^{4+} ions are expected to occupy all three of these sites. The remaining 6 Ce^{4+} and the 12 Ce^{3+} then occupy the Ce(2) which leads to a similar problem as already noted for Ce_3O_5 above. When the BVM and IHMA results are compared, we notice that the BVM predicts that there are two distinct valences for the Ce ions, one closer to Ce^{3+} and the other closer to Ce^{4+} but without the inconsistency of assigning different valences to the same type of Ce site. These results indicate mixed valence in Ce_7O_{12}.

E. $Ce_{11}O_{20}$

This oxide has the lowest crystal symmetry of all the cerium oxides included in this study. Based on the BVM results in Table I, the following approximate assignments of site oxidation states can be made: Ce(1) and Ce(2): Ce^{3+}; Ce(3) and Ce(4): strongly mixed valent; and Ce(5) and Ce(6): closer to Ce^{4+} but still mixed valent. Figure 3 shows that the

TABLE III. Bond length data used in the bond valence calculations of the Ce oxides. Crystallographic data were obtained from the references as cited in the table and the Ce-O bond lengths were calculated from that data in CRYSTALMAKER® (Ref. 77). The O atoms, $O(i)(i=1-8)$ in each polyhedron may be equivalent or distinct O sites in a given crystal. All bond lengths are in angstrom. Estimated errors in bond lengths are approximately ±0.01 Å.

Oxide	Ref.	Ce Site	Bond Lengths in Ce Coordination Polyhedron[a]							
			O(1)	O(2)	O(3)	O(4)	O(5)	O(6)	O(7)	O(8)
A-Ce_2O_3	82 and 83	Ce	2.339	2.339	2.339	2.434	2.694	2.694	2.694	
C-Ce_2O_3	83–85	Ce(1)	2.404	2.404	2.404	2.404	2.404	2.404		
		Ce(2)	2.370	2.370	2.422	2.422	2.455	2.455		
Ce_3O_5	83, 85, and 86	Ce(1)	2.381	2.381	2.381	2.381	2.381	2.381	2.600	2.600
		Ce(2)	2.347	2.347	2.398	2.398	2.431	2.431	2.468	2.468
Ce_7O_{12}	87 and 88	Ce(1)	2.249	2.249	2.249	2.249	2.249	2.249		
		Ce(2)	2.405	2.392	2.652	2.307	2.367	2.380	2.478	
$Ce_{11}O_{20}$	85 and 89	Ce(1)	2.489	2.474	2.379	2.489	2.474	2.379	2.701	2.701
		Ce(2)	2.423	2.407	2.446	2.624	2.589	2.444	2.539	2.597
		Ce(3)	2.311	2.405	2.263	2.333	2.447	2.385	2.379	
		Ce(4)	2.251	2.309	2.361	2.544	2.267	2.279	2.356	
		Ce(5)	2.429	2.254	2.268	2.342	2.240	2.358	2.281	
		Ce(6)	2.214	2.280	2.227	2.315	2.306	2.274	2.429	
Ce_6O_{11}	80, 84, and 90	Ce(1)	2.180	2.241	2.245	2.490	2.560	2.618		
		Ce(2)	2.189	2.230	2.236	2.252	2.516	2.669	2.834	
		Ce(3)	2.260	2.324	2.377	2.441	2.593	2.603	2.698	
		Ce(4)	2.064	2.143	2.147	2.189	2.670			
		Ce(5)	2.235	2.285	2.347	2.482	2.723	2.830		
		Ce(6)	2.180	2.241	2.245	2.490	2.590	2.618		
CeO_2	80, 84, and 91	Ce	2.343	2.343	2.343	2.343	2.343	2.343	2.343	2.343

[a]Only the bond lengths satisfying the Brown-Altermatt criterion for the coordination polyhedra are shown (Ref. 73).

HMA predicts a valence of 3.6 v.u. which is also mixed valent. The ionic formulation $[(Ce^{3+})_4(Ce^{4+})_7](O^{-2})_{20}$ results from applying the IHMA to this crystal. Both the BVM and the IHMA predict the presence of Ce^{3+} sites in this crystal, and a consistent distribution of the sites is obtained between the methods since it is expected that, in the IHMA ionic formulation, the larger Ce^{3+} ion will occupy the larger eight-coordinated polyhedra Ce(1) and Ce(2) which is the same result obtained from the BVM analysis. However, the two methods disagree on the assignment of valencies to the remainder of the sites with the IHMA assigning them all to Ce^{4+} while the BVM clearly indicates strong mixed valence for the Ce(3) and Ce(4) sites and less but still significant mixed valence for the Ce(5) and Ce(6) sites. The HMA does not appear to be a viable proposition for this crystal lattice because of its very low symmetry. Again, we find that $Ce_{11}O_{20}$ is a mixed-valence compound, but one that does not fit into either of the traditional classes.

F. Ce_6O_{11}

The results in Table I obtained from the BVM show that all Ce sites in Ce_6O_{11} are mixed valent with deviations from the nearest integral valences increasing from 0.1 to 0.38 v.u. in the order Ce(5), Ce(3), Ce(1), Ce(6), Ce(2), and Ce(4). We however note that the delineation of the Ce polyhedra was ambiguous in all of the six Ce polyhedra in the crystal of this oxide.

When the Brown-Altermatt criterion[73] was applied to the various Ce sites, several marginal bonds were excluded from the first coordination shell and thus from the bond valence sums. Table IV, as discussed in Appendix B, shows the amounts by which respective bond valence sums would change if the marginal bonds were included in the bond valence sums.

As shown in Fig. 3, the HMA predicts mixed valence for this compound giving a valence of 3.7 v.u. for the Ce ions. Considered in the IHMA, the ionic composition of Ce_6O_{11} would be $[(Ce^{3+})_2(Ce^{4+})_4](O^{2-})_{11}$ which implies that there are twice as many Ce^{4+} ion sites as Ce^{3+} sites in a unit cell of Ce_6O_{11}. We notice that the predictions of the three methods are very different for this crystal. Table I shows that this crystal has the most distorted polyhedra with percent variation in the bond lengths ranging from 15 to 37%, and it is expected that the BVM would reflect this aspect of the local site geometries. With these complex local geometries, it is not expected that the HMA would give a good approximation to the site valences. Comparing the IHMA and the BVM, we notice that even if one tentatively considered both Ce(2) and Ce(4) to be Ce^{4+} sites and the rest is Ce^{3+}, then one gets twice as many Ce^{3+} sites as Ce^{4+} sites. This charge ordering is the reverse of that predicted by the IHMA ionic formula-

tion which clearly highlights the disagreement between the methods.

G. CeO_2

Our value of $N_f=0.27$ for CeO_2 is comparable to the result obtained by Castleton *et al.*[99] from an LDA+U calculation as shown in Table II. Table II shows that results from 3d core-level spectroscopy tend to give relatively high N_f values ($N_f \geq 0.40$). In CeO_2, the Ce site is in a symmetric polyhedron with all the Ce-O bonds equal in length, and therefore the bond valence model is expected to perform well for this oxide. As can be seen from Fig. 3, the HMA predicts that the Ce ion is in a pure f^0 configuration in CeO_2. The same result is obtained from the IHMA, and thus both methods contradict the BVM. From our result, we conclude that CeO_2 is a mixed-valent compound.

It would be informative to compare the bond valence-sum results obtained here to those for their Pr oxide counterparts. However, we have not found any detailed study on the bond valence sums of Pr oxides for a meaningful comparison to be made here. We only found a bond valence calculation performed for the Pr-O bond in the high-T_c superconductor $PrYBa_2Cu_3O_7$ where the Pr was mixed valent with a valence of 3.4 v.u.[103]

V. CONCLUSION

Since we did not obtain integral N_f values for most of the Ce oxide sites, our results suggest that mixed valence is an essential feature of Ce in its pure oxide phases. We have also shown that for a given crystallographic phase, several different oxidation states may exist for Ce sites which belong to the same point group. Thus, it appears that valence fluctuations depend on the exact coordination geometry of a Ce site which suggests that valence fluctuation is a "local" property of the Ce site. The point group symmetry of a Ce site does not appear to play a significant role in determining the valence state of that site. We have also noted that the bond valence method eliminates some of the conceptual difficulties which arise when one attempts to distribute Ce ions of different integral valences in sites of the same type in a given crystal.

ACKNOWLEDGMENTS

Our interest in the study of cerium oxides was motivated by our discussions with C. Stampfl at the University of Sydney. We thank B. Powell, A. Jacko, E. Scriven, J. Merino, M. Yethiraz, A. Stilgoe, B. Mostert, and H. F. Schaefer for helpful discussions. One of us (E.S.) is grateful to the Australian Commonwealth Government Department of Science Education and Training, and to the University of Queensland, for support. This work was also supported by the Australian Research Council.

TABLE IV. Marginal bond valences for Ce_6O_{11} according to the Brown-Altermatt criterion (Ref. 73).

Ce coord. polyhedron	Marginal bond length Å	Calculated bond valence (v.u.)
Ce(1)	2.944	0.052
	3.695	0.007
Ce(2)	3.561	0.009
Ce(3)	3.594	0.010
	3.658	0.008
Ce(4)	2.976	0.010
	2.980	0.008
Ce(5)	3.049	0.045
	3.114	0.037
Ce(6)	2.944	0.052
	2.999	0.044
	3.640	0.008
	3.699	0.006

APPENDIX A: BOND LENGTHS IN THE VARIOUS CERIUM COORDINATION POLYHEDRA OF THE CERIUM OXIDES

The calculated Ce-O bond distances in the various Ce coordination polyhedra of the Ce oxide crystals are listed in Table III.

APPENDIX B: BOND VALENCES OF THE MARGINAL BONDS IN THE DELINEATION OF Ce COORDINATION POLYHEDRA IN Ce_6O_{11}

Table IV lists all the bonds whose lengths are just outside the threshold values as determined from the Brown-Altermatt criterion[73] for delineating the coordination polyhedra and were thus excluded from the bond valence sums given in Table I. The respective bond valences have been calculated and included in Table IV. Adding these to the corresponding bond valence sums of Table I indicates how much the bond valence sums would change if these bonds are included in the Ce coordination polyhedra. Their effect would be small.

[1] R. McWeeney, *Coulson's Valence* (Oxford, New York, 1980).
[2] For a recent survey, see R. J. H. Clark, P. Day, and N. S. Hush, Philos. Trans. R. Soc. London, Ser. A **366**, 3 (2008).
[3] M. Robin and P. Day, Adv. Inorg. Chem. Radiochem. **10**, 247 (1967).
[4] P. Cox, *The Electronic Structure and Chemistry of Solids, Section 6.3* (Oxford University Press, Oxford, 1987).
[5] C. M. Varma, Rev. Mod. Phys. **48**, 219 (1976).
[6] W. E. Gardner, J. Penfold, T. F. Smith, and I. R. Harris, J. Phys. F **2**, 133 (1972).
[7] B. Batlogg, H. R. Ott, E. Kaldis, W. Thoni, and P. Wachter, Phys. Rev. B **19**, 247 (1979).

[8] D. T. Adroja and S. K. Malik, J. Magn. Magn. Mater. **100**, 126 (1991).
[9] F. Walz, J. Phys.: Condens. Matter **14**, R285 (2002).
[10] B. Batlogg, E. Kaldis, A. Schlegel, and P. Wachter, Phys. Rev. B **12**, 3940 (1975).
[11] H. Ohara, S. Sasaki, Y. Konoike, T. Toyoda, K. Yamawaki, and M. Tanaka, Physica B **350**, 353 (2004).
[12] P. Ravindran, R. Vidya, H. Fjellvag, and A. Kjekshus, Phys. Rev. B **77**, 134448 (2008).
[13] A. Trovarelli, *Catalysis by Ceria and Related Materials* (Imperial College Press, London, 2002).
[14] B. F. Hoskins and R. L. Martin, Aust. J. Chem. **48**, 709 (1995).
[15] N. V. Skorodumova, S. I. Simak, B. I. Lundqvist, I. A. Abrikosov, and B. Johansson, Phys. Rev. Lett. **89**, 166601 (2002).
[16] F. Esch, S. Fabris, L. Zhou, T. Montini, C. Africh, P. Fornasiero, G. Comelli, and R. Rosei, Science **309**, 752 (2005).
[17] I. D. Brown, Acta Crystallogr. B **48**, 553 (1992).
[18] I. D. Brown, *The Chemical Bond in Inorganic Chemistry: The Bond Valence Model, International Union of Crystallography* (Oxford Science, London, 2002).
[19] J. K. Burdett, *Chemical Bonding in Solids* (Oxford University Press, London, 1995), Chap. 6.
[20] A. Kotani, T. Jo, and J. C. Parlebas, Adv. Phys. **37**, 37 (1988).
[21] J. M. Lawrence, P. S. Riseborough, and R. D. Parks, Rep. Prog. Phys. **44**, 1 (1981).
[22] A. Kotani and H. Ogasawasara, J. Electron Spectrosc. Relat. Phenom. **60**, 257 (1992).
[23] F. de Groot and A. Kotani, *Core Level Spectroscopy of Solids, Advances in Condensed Matter Science* (CRC, Boca Raton, FL, 2008).
[24] E. Wuilloud, B. Delley, W.-D. Schneider, and Y. Baer, Phys. Rev. Lett. **53**, 202 (1984).
[25] T. Jo and A. Kotani, Solid State Commun. **54**, 451 (1985).
[26] A. Kotani, H. Mizuta, T. Jo, and J. C. Parlebas, Solid State Commun. **53**, 805 (1985).
[27] M. Nakazawa, S. Tanaka, T. Uozumi, and A. Kotani, J. Phys. Soc. Jpn. **65**, 2303 (1996).
[28] A. Fujimori, Phys. Rev. B **28**, 2281 (1983).
[29] A. Fujimori, Phys. Rev. B **27**, 3992 (1983).
[30] M. V. R. Rao and T. Shripathi, J. Electron Spectrosc. Relat. Phenom. **87**, 121 (1997).
[31] A. V. Soldatov, T. S. Ivanchenko, S. Della Longa, A. Kotani, Y. Iwamoto, and A. Bianconi, Phys. Rev. B **50**, 5074 (1994).
[32] H. Dexpert, R. C. Karnatak, J. M. Esteva, J. P. Connerade, M. Gasgnier, P. E. Caro, and L. Albert, Phys. Rev. B **36**, 1750 (1987).
[33] A. Bianconi, A. Marcelli, H. Dexpert, R. Karnatak, A. Kotani, T. Jo, and J. Petiau, Phys. Rev. B **35**, 806 (1987).
[34] R. C. Karnatak, J. M. Esteva, H. Dexpert, M. Gasgnier, P. E. Caro, and L. Albert, J. Magn. Magn. Mater. **63-64**, 518 (1987).
[35] A. Bianconi, M. Campagna, and S. Stizza, Phys. Rev. B **25**, 2477 (1982).
[36] L. D. Finkelstein, A. V. Postnikov, N. N. Efremova, and E. Z. Kurmaev, Mater. Lett. **14**, 115 (1992).
[37] G. Krill, J. P. Kappler, A. Meyer, L. Abadli, and M. F. Ravet, J. Phys. F: Met. Phys. **11**, 1713 (1981).
[38] A. Kotani, M. Okada, and T. Jo, J. Phys. Soc. Jpn. **56**, 798 (1987).
[39] R. Haensel, P. Rabe, and B. Sonntag, Solid State Commun. **8**, 1845 (1970).
[40] T. Hanyu, H. Ishii, M. Yanagihara, T. Kamada, T. Miyahara, H. Kato, K. Naito, S. Suzuki, and T. Ishii, Solid State Commun. **56**, 381 (1985).
[41] T. Miyahara, A. Fujimori, T. Koide, S. Sato, S. Shin, Y. O. M. Ishigame, and T. Komatsubara, J. Phys. Soc. Jpn. **56**, 3689 (1987).
[42] M. Matsumoto, K. Soda, K. Ichikawa, S. Tanaka, Y. Taguchi, K. Jouda, O. Aita, Y. Tezuka, and S. Shin, Phys. Rev. B **50**, 11340 (1994).
[43] S. M. Butorin *et al.*, Phys. Rev. Lett. **77**, 574 (1996).
[44] T. K. Sham, R. A. Gordon, and S. M. Heald, Phys. Rev. B **72**, 035113 (2005).
[45] J. W. Allen, J. Magn. Magn. Mater. **47-48**, 168 (1985).
[46] A. F. Orchard and G. Thornton, J. Electron Spectrosc. Relat. Phenom. **10**, 1 (1977).
[47] M. V. Ryzhkov, V. A. Gubanov, Y. A. Teterin, and A. S. Baev, Z. Phys. B: Condens. Matter **59**, 1 (1985).
[48] T. Nakano, A. Kotani, and J. C. Parlebas, J. Phys. Soc. Jpn. **56**, 2201 (1987).
[49] T. Jo and A. Kotani, Phys. Rev. B **38**, 830 (1988).
[50] D. D. Koelling, A. M. Boring, and J. H. Wood, Solid State Commun. **47**, 227 (1983).
[51] G. Thornton and M. J. Dempsey, Chem. Phys. Lett. **77**, 409 (1981).
[52] P. J. Hay, R. L. Martin, J. Uddin, and G. E. Scuseria, J. Chem. Phys. **125**, 034712 (2006).
[53] D. A. Andersson, S. I. Simak, B. Johansson, I. A. Abrikosov, and N. V. Skorodumova, Phys. Rev. B **75**, 035109 (2007).
[54] S. Fabris, S. de Gironcoli, S. Baroni, G. Vicario, and G. Balducci, Phys. Rev. B **71**, 041102(R) (2005).
[55] N. V. Skorodumova, R. Ahuja, S. I. Simak, I. A. Abrikosov, B. Johansson, and B. I. Lundqvist, Phys. Rev. B **64**, 115108 (2001).
[56] J. L. F. Da Silva, Phys. Rev. B **76**, 193108 (2007).
[57] M. Nolan, S. Grigoleit, D. C. Sayle, S. C. Parker, and G. W. Watson, Surf. Sci. **576**, 217 (2005).
[58] J. L. F. Da Silva, M. V. Ganduglia-Pirovano, J. Sauer, V. Bayer, and G. Kresse, Phys. Rev. B **75**, 045121 (2007).
[59] E. N. Brothers, A. F. Izmaylov, J. O. Normand, V. Barone, and G. E. Scuseria, J. Chem. Phys. **129**, 011102 (2008).
[60] G. Kotliar, S. Y. Savrasov, K. Haule, V. S. Oudovenko, O. Parcollet, and C. A. Marrianetti, Rev. Mod. Phys. **78**, 865 (2006).
[61] L. V. Pourovskii, B. Amadon, S. Biermann, and A. Georges, Phys. Rev. B **76**, 235101 (2007).
[62] F. Mohri, Acta Crystallogr. **59**, 190 (2003).
[63] N. E. Brese and M. O'Keeffe, Acta Crystallogr., Sect. B: Struct. Sci. **47**, 192 (1991).
[64] A. Trzesowska, R. Kruszynski, and T. Bartczak, Acta Crystallogr. **60**, 174 (2004).
[65] C. Ferraris, *Fundamentals of Crystallography* (Oxford University Press, London, 2002).
[66] U. Mueller, *Inorganic Structural Chemistry* (John Wiley & Sons, New York, 1993).
[67] R. Hoppe, Z. Kristallogr. **150**, 23 (1979).
[68] R. Hoppe, Angew. Chem., Int. Ed. Engl. **9**, 25 (1970).
[69] F. L. Carter, Acta Crystallogr., Sect. B: Struct. Crystallogr. Cryst. Chem. **34**, 2962 (1978).
[70] R. Hoppe, S. Voight, H. Glaum, J. Kissel, H. P. Mueller, and K. Bernet, J. Less- Common Met. **156**, 105 (1989).
[71] M Attarian Shandiz, J. Phys.: Condens. Matter **20**, 325237

(2008).
[72] I. Brown, *The Chemical Bond in Inorganic Chemistry: The Bond Valence Model* (Oxford Science, London, 2002), Chap. 4, p. 43.
[73] D. Altermatt and I. D. Brown, Acta Crystallogr., Sect. B: Struct. Sci. **41**, 240 (1985).
[74] P. L. Roulhac and G. J. Palenik, Inorg. Chem. **42**, 118 (2003).
[75] F. Zocchi, J. Mol. Struct.: THEOCHEM **805**, 73 (2007).
[76] F. Zocchi, Solid State Sci. **4**, 149 (2002).
[77] CrystalMaker®, A Crystal and Molecular Structures Program for Mac and Windows (2008).
[78] L. Eyring, in *Handbook on the Physics and Chemistry of Rare Earths*, edited by K. A. Gschneider and L. Eyring (Elsevier, New York, 1979), Vol. 3, p. 27.
[79] S. Tsunekawa, R. Sivamohan, S. Ito, A. Kasuya, and T. Fukuda, Nanostruct. Mater. **11**, 141 (1999).
[80] O. T. Sorensen, J. Solid State Chem. **18**, 217 (1976).
[81] G. Meyer and H. J. Meyer, Chem. Mater. **4**, 1157 (1992).
[82] H. Barnighausen and G. Schiller, J. Less- Common Met. **110**, 385 (1985).
[83] R. W. G. Wyckoff, *Crystal Structures*, 2nd ed. (Interscience, New York, 1963), Vol. 2.
[84] P. Villars and L. D. Calvert, *Pearson's Handbook of Crystallographic Data for Intermetallic Phases* (ASM International, New York, 1991), Vol. 2.
[85] E. A. Kummerle and G. Heger, J. Solid State Chem. **147**, 485 (1999).
[86] M. Zinkevich, D. Djurovic, and F. Aldinger, Solid State Ionics **177**, 989 (2006).
[87] S. F. Bartram, Inorg. Chem. **5**, 749 (1966).
[88] S. P. Ray and D. E. Cox, J. Solid State Chem. **15**, 333 (1975).
[89] J. Zhang, R. V. Dreele, and L. Eyring, J. Solid State Chem. **104**, 21 (1993).
[90] J. Zhang, R. B. Von Dreele, and L. Eyring, J. Solid State Chem. **122**, 53 (1996).
[91] D. Taylor, Br. Ceram. Trans. J. **83**, 32 (1984).
[92] I. D. Brown, *The Bond-valence Method: An Empirical Approach to Chemical Structure and Bonding* (Academic, New York, 1981), Vol. II, Chap. 1, pp. 1–30.
[93] A. J. Locock and P. C. Burns, Z. Kristallogr. **219**, 259 (2004).
[94] S. V. Krivovichev and I. D. Brown, Z. Kristallogr. **216**, 245 (2001).
[95] F. Liebau and X. Wang, Z. Kristallogr. **220**, 589 (2005).
[96] Z. Wu, R. E. Benfield, L. G. H. Li, Q. Yang, D. Grandjean, Q. Li, and H. Zhu, J. Phys.: Condens. Matter **13**, 5269 (2001).
[97] J. Roehler, *Handbook on the Physics and Chemistry of Rare Earths* (Elsevier Science, New York, 1987), Chap. 71, pp. 453–545.
[98] F. Marabelli and P. Wachter, Phys. Rev. B **36**, 1238 (1987).
[99] C. W. M. Castleton, J. Kullgren, and K. Hermansson, J. Chem. Phys. **127**, 244704 (2007).
[100] A. Kotani, H. Ogasawara, K. Okada, B. T. Thole, and G. A. Sawatzky, Phys. Rev. B **40**, 65 (1989).
[101] S. Arai, S. Muto, J. Murai, T. Sasaki, Y. Ukyo, K. Kuroda, and H. Saka, Mater. Trans. **45**, 2951 (2004).
[102] R. D. Shannon, Acta Crystallogr., Sect. B: Struct. Crystallogr. Cryst. Chem. **32**, 751 (1976).
[103] M. Guillaume, P. Allenspach, J. Mesot, B. Roessli, U. Staub, P. Fischer, and A. Furrer, Z. Phys. B: Condens. Matter **90**, 13 (1993).